Journal of Alloys and Compounds 729 (2017) 742–748

Contents lists available at ScienceDirect

Journal of Alloys and Compounds

journal homepage: http://www.elsevier.com/locate/jalcom

Correlation between vibrational modes of A-site ions and microwave dielectric properties in $(1-x)\ CaTiO_3-x\ (Li_{0.5}Sm_{0.5})TiO_3$ ceramics

Fanfan Ning [a], Lin Gan [a], Shifeng Yuan [a], Zeming Qi [b], Juan Jiang [a, *], Tianjin Zhang [a, **]

[a] Hubei Collaborative Innovation Center for Advanced Organic Chemical Materials, Ministry of Education Key Laboratory for the Green Preparation and Application of Functional Materials and School of Material Science and Engineering, Hubei University, Wuhan 430062, China
[b] National Synchrotron Radiation Laboratory, University of Science and Technology of China, Hefei 230029, China

ARTICLE INFO

Article history:
Received 30 July 2017
Received in revised form
16 September 2017
Accepted 18 September 2017
Available online 20 September 2017

Keywords:
Microwave dielectric properties
Raman
Infrared reflection
Vibrational modes

ABSTRACT

$(1-x)CaTiO_3-x(Li_{0.5}Sm_{0.5})TiO_3$ ($0.7 \leq x \leq 0.8$, CLST) ceramics with an orthorhombic perovskite structure were fabricated by a conventional solid-state reaction method. The effects of composition variation on the microwave dielectric properties were studied in detail. The permittivity (ε_r) and quality factor ($Q \times f$) value decreased with an increase in the x value, and the temperature coefficient of the resonant frequency (τ_f) reached nearly zero. Raman and infrared reflection spectroscopy were employed to reveal the relationship between vibrational modes and microwave dielectric properties. The Raman spectra fitted with the Lorentzian model indicated that the dielectric loss deteriorates with an increase in the x value are the result of the lowered A-site cation ordering degree. The harmonic oscillator model was used to fit the infrared reflection spectra, and the obtained complex dielectric response was extrapolated down to the microwave region. The infrared reflection spectra show that the vibrational modes related to A-site cations at lower frequencies (i.e., <150 cm^{-1}) play the most important role in the microwave dielectric properties of CLST ceramics. The optimal microwave dielectric properties were found to be $\varepsilon_r = 109.4$, $Q \times f = 4698$ GHz, and $\tau_f = 1.6$ ppm/°C in the sample of $0.22CaTiO_3$-$0.78(Li_{0.5}Sm_{0.5})TiO_3$.

1. Introduction

In recent years, with the rapid development of wireless communication and satellite communication, microwave dielectric ceramics have been intensively studied because of their popular applications in the fields of global positioning system (GPS) and wireless local area network (WLAN) technology. It is known that miniaturization, integration, and high reliability are important requirements for microwave electronic devices and portable terminals. Therefore, to fabricate high-performance microwave dielectric ceramics for the applications mentioned above, a high dielectric constant (ε_r), outstanding quality factor ($Q \times f$), and near-zero temperature coefficient of resonant frequency (τ_f) are necessary to achieve component miniaturization, good signal recognition, and excellent temperature stability [1–3].

In general, it is quite challenging to fabricate microwave dielectric ceramics that simultaneously satisfy the three required characteristics for microwave dielectric applications because materials with high permittivity usually have a high dielectric loss and a large τ_f. In previous studies, a series of microwave dielectric ceramics with high ε_r, such as A-site-modified perovskite (A+ 1/2A3+ 1/2)TiO_3, tungsten bronze-type BaO-Ln_2O_3-TiO_2, complex perovskite CaO-Li_2O-Ln_2O_3-TiO_2 or $CaTiO_3$-$(Li_{0.5}Ln_{0.5})TiO_3$, and Pb-based ceramics have been developed [4–7]. Unfortunately, the high sintering temperatures of tungsten bronze-type and Pb-based materials, and the large positive τ_f values of some of the A-site-modified perovskites, hinder the application of these microwave dielectric ceramics. Solid solutions of $(1-x)CaTiO_3-x(Li_{0.5}Ln_{0.5})TiO_3$ (Ln = Nd, Sm, La) present promising microwave dielectric properties, which include high ε_r, superior $Q \times f$ values, and adjustable temperature coefficient of resonant frequency [8–10]. $CaTiO_3$-$(Li_{1/2}Ln_{1/2})TiO_3$-based solid solutions were first reported by Ezaki et al. [6], and temperature-stable dielectric ceramics can be obtained in a CaO-Li_2O-Ln_2O_3-TiO_2 system with $\varepsilon_r = 110$, $Q \times f = 4500$ GHz, and $\tau_f = 7.0$ ppm/°C. Kim et al. [8] reported the dielectric properties of the $(1-x)CaTiO_3-x(Li_{0.5}Sm_{0.5})TiO_3$ system, which exhibits values of $\varepsilon_r = 114$, $Q \times f = 3700$ GHz, and $\tau_f = 11.5$ ppm/°C for $x = 0.7$. Li et al.

* Corresponding author.
** Corresponding author.
E-mail addresses: jiangjuan@hubu.edu.cn (J. Jiang), zhangtj@hubu.edu.cn (T. Zhang).

https://doi.org/10.1016/j.jallcom.2017.09.198
0925-8388/

[11] reported that $Ca_{1-x}(Li_{1/2}Sm_{1/2})_xTiO_3$ ceramics had good performance, with microwave dielectric properties of $\varepsilon_r = 105.8$, $Q \times f = 3170$ GHz, and $\tau_f = 0$ ppm/°C when x = 0.75. Gu et al. [12] found that $0.2Ca_{0.8}Sr_{0.2}TiO_3$-$0.8(Li_{0.5}Sm_{0.5})TiO_3$ solid solution ceramics exhibit good microwave dielectric properties of $\varepsilon_r = 113$, $Q \times f = 4400$ GHz, and $\tau_f = 8.4$ ppm/°C.

Although much work has been done to control the microwave dielectric properties of materials that are based on $CaTiO_3$-$(Li_{0.5}Sm_{0.5})TiO_3$ ceramics, a fundamental principles study on the permittivity and dielectric losses in solid solution is still needed to reveal the responsible mechanism. The dielectric properties of microwave dielectric ceramics mostly depend on ionic polarization caused by lattice vibrations. Therefore, Raman and infrared spectroscopy are usually considered useful tools to study the relationship between the dielectric properties and the vibrational modes [13–15]. Dielectric losses include an intrinsic part and extrinsic part. The intrinsic losses may be obtained from the infrared reflection spectra using the classical harmonic oscillator model [16]. In addition, the Raman spectra may reveal the short-range characteristics of the ceramics, including order-disorder transitions [17]. Zhou et al. [18–20] reported that the Far-infrared spectra (50–1000 cm-1) study showed that complex dielectric spectra were in good agreement with the measured microwave permittivity and dielectric losses in $(Na_{0.5}La_{0.5})MoO_4$-$(Na_{0.5}Bi_{0.5})MoO_4$ ceramics. They also reported that the infrared spectra showed that the external vibrations of $CeVO_4$ had the most remarkable effects on the dielectric constant in the $CeVO_4$-TiO_2 composite ceramics. In addition, the Raman, infrared reflection, and terahertz spectra of A-site-deficient scheelite materials $(Ca_{1-3x}Bi_{2x}\Phi_x)MoO_4$(Φ: A-site vacancy) were studied to evaluate the correlation between the vibrational modes and the microwave dielectric properties.

In this work, a series of $(1-x)CaTiO_3$-$x(Li_{0.5}Sm_{0.5})TiO_3$ ($0.7 \le x \le 0.8$, CLST) ceramics were synthesized by a solid-state reaction method. The effects of compositional variation on the structure and microwave dielectric properties of the samples were investigated in detail. Additionally, the relationship between vibrational modes and microwave dielectric properties was discussed by fitting the Raman and the infrared reflection spectra.

2. Experimental procedure

$(1-x)CaTiO_3$-$x(Li_{0.5}Sm_{0.5})TiO_3$ ($0.7 \le x \le 0.8$, CLST) ceramics were prepared by the conventional solid-state reaction method from commercial powders of $CaCO_3$(99.0%), TiO_2(99.9%), Li_2CO_3(99.9%), and Sm_2O_3(99.99%). Initially, stoichiometric ratios of $CaCO_3$ and TiO_2, and Li_2CO_3, Sm_2O_3, and TiO_2, were respectively mixed using ethanol medium and ZrO_2 balls for 12 h. After drying, $CaTiO_3$ was calcined at 1090 °C for 5 h and $(Li_{0.5}Sm_{0.5})TiO_3$ was calcined at 1100 °C for 3 h. Then, the calcined powders were weighed according to the compositions of $(1-x)CaTiO_3$-$x(Li_{0.5}Sm_{0.5})TiO_3$ ($x = 0.70, 0.72, 0.74, 0.76, 0.78, 0.80$) and were milled again for 12 h in ethanol medium. The powers were mixed with 10 wt% polyvinyl alcohol (PVA, 5%) solution as a binder after drying and were uniaxially pressed into pellets 12 mm in diameter and 6–7 mm in thickness. Finally, the pellets were heated at 550 °C for 3 h to eliminate the binder and then sintered at 1240 °C for 4 h in air.

The crystal structure of the sintered samples was analyzed using X-ray powder diffraction (XRD, D8 advance, Bruker, Germany) with Cu Kα radiation. The microstructures of the ceramics were observed using a scanning electron microscope (SEM, JSM-7100F, JEOL, Japan). The Raman spectra were recorded at room temperature using a Raman spectrometer (inVia, Renishaw, UK) excited with an Ar ion laser (633 nm). The infrared reflection spectra were measured using a Bruker IFS 66v FTIR spectrometer (Bruker Optics, Ettlingen, Germany) on the infrared beamline station (U4) at the National Synchrotron Radiation Lab. (NSRL), China. Microwave dielectric properties of the ceramics were measured with the $TE_{01\delta}$ shielded cavity reflection method with a network analyzer (E5071C, Agilent, Palo Alto, CA). The temperature coefficient of the resonant frequency (τ_f) was measured at −20 °C and 65 °C and was calculated using the following formula (Eq. (1)):

$$\tau_f = \frac{f_{(T_2)} - f_{(T_1)}}{f_{(T_1)}(T_2 - T_1)} \times 10^6 \ \ (\text{ppm/°C}) \tag{1}$$

where $f_{(T_1)}$ and $f_{(T_2)}$ represent the resonant frequencies measured at −20 °C and 65 °C, respectively.

3. Results and discussion

Fig. 1 shows the XRD patterns of the CLST ceramics with various compositions. All diffraction peaks were indexed as an orthorhombic perovskite structure (JCPDS card No. 42-0423, $CaTiO_3$, space group *Pmna*), and no secondary phases were observed in all compositions. This result indicates that $(Li_{0.5}Sm_{0.5})^{2+}$ ions have diffused into $CaTiO_3$ lattices and formed a solid solution. Furthermore, the diffraction peaks shift to a higher angle as *x* increases, suggesting that the unit cell volume of the solid solution gradually decreases with an increase in the *x* value as a result of the partial substitution of the smaller A-site ionic radii of $(Li_{0.5}Sm_{0.5})^{2+}$ ions (0.9995 Å) for larger Ca^{2+} ions (1.1200 Å) [21].

Fig. 2 shows SEM images of the surfaces of the CLST ceramics with various compositions after hot corrosion treatment. A well-densified microstructure was observed and there was no obvious secondary phase for all compositions, which agreed well with the XRD patterns. The average grain size of the samples was in the range of 1–4 μm. The SEM observations suggest that there is no significant difference in the microstructure of samples with various compositions. In addition, the relative densities of the CLST ceramics are very high (i.e., about 97%). And the relative density is almost constant with the change of composition.

Fig. 3 presents the microwave dielectric properties of the CLST ceramics as a function of the *x* value. In Fig. 3(a), the permittivity decreases monotonously as the *x* value increases from 0.70 to 0.80, which is in a good agreement with the results of Kim et al. [8] and Li et al. [11]. A possible reason is that $(Li_{0.5}Sm_{0.5})^{2+}$ has a smaller ionic polarizability (2.97 $Å^3$) than that of Ca^{2+} (3.16 $Å^3$) [22], the ionic polarizability of the CLST ceramics decreased with the increase of *x* value. According to Clausius-Mossotti equation, the ionic polarizability is directly proportional to the dielectric constant [23]. Therefore, the permittivity is dependent on the ionic polarizability, and a decrease in the ionic polarizability leads to a decrease in the permittivity. In addition, the variation of permittivity with *x* value in this study may be associated with the change in the lattice vibration mode caused by the substitution of A-site ions, as will be discussed later in the infrared spectroscopy analysis.

The $Q \times f$ value of the CLST samples also shows a downward trend with an increase in the *x* value, as seen in Fig. 3(b). It is widely known that the $Q \times f$ value depends on extrinsic factors such as the secondary phase, impurity, grain size, and density, as well as intrinsic losses related to the lattice vibration modes [24]. However, the effects of extrinsic factors on the $Q \times f$ value may be negligible, as on one hand no secondary phase or impurities were detected by the XRD analysis (see Fig. 1), and on the other hand, dense microstructures and fine grain sizes were observed in the SEM images (see Fig. 2). Therefore, the decrease in the $Q \times f$ value with *x* value may be attributed to the intrinsic losses caused by the variation in the lattice vibration mode.

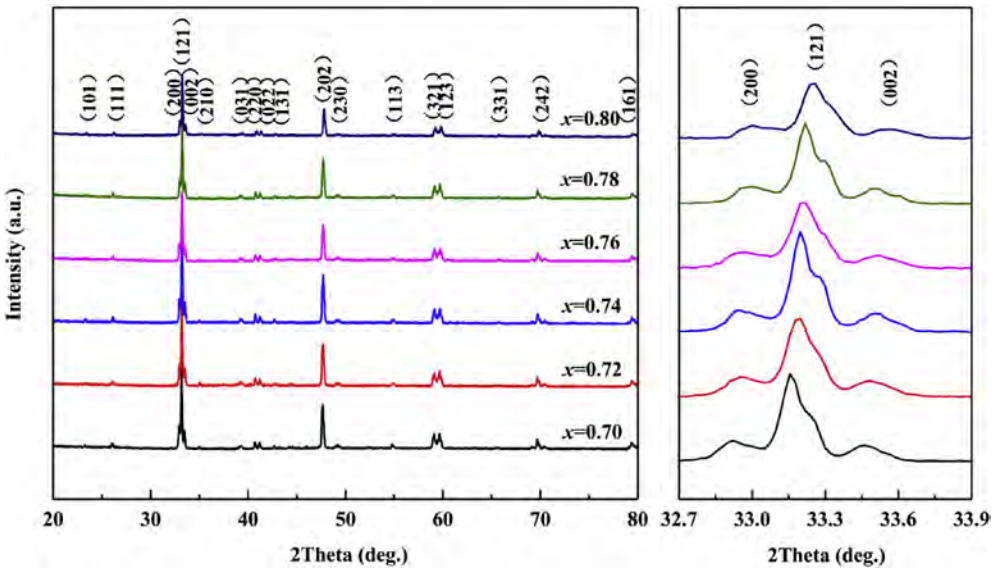

Fig. 1. XRD patterns of $(1-x)CaTiO_3-x(Li_{0.5}Sm_{0.5})TiO_3$ ($0.70 \le x \le 0.80$) ceramics.

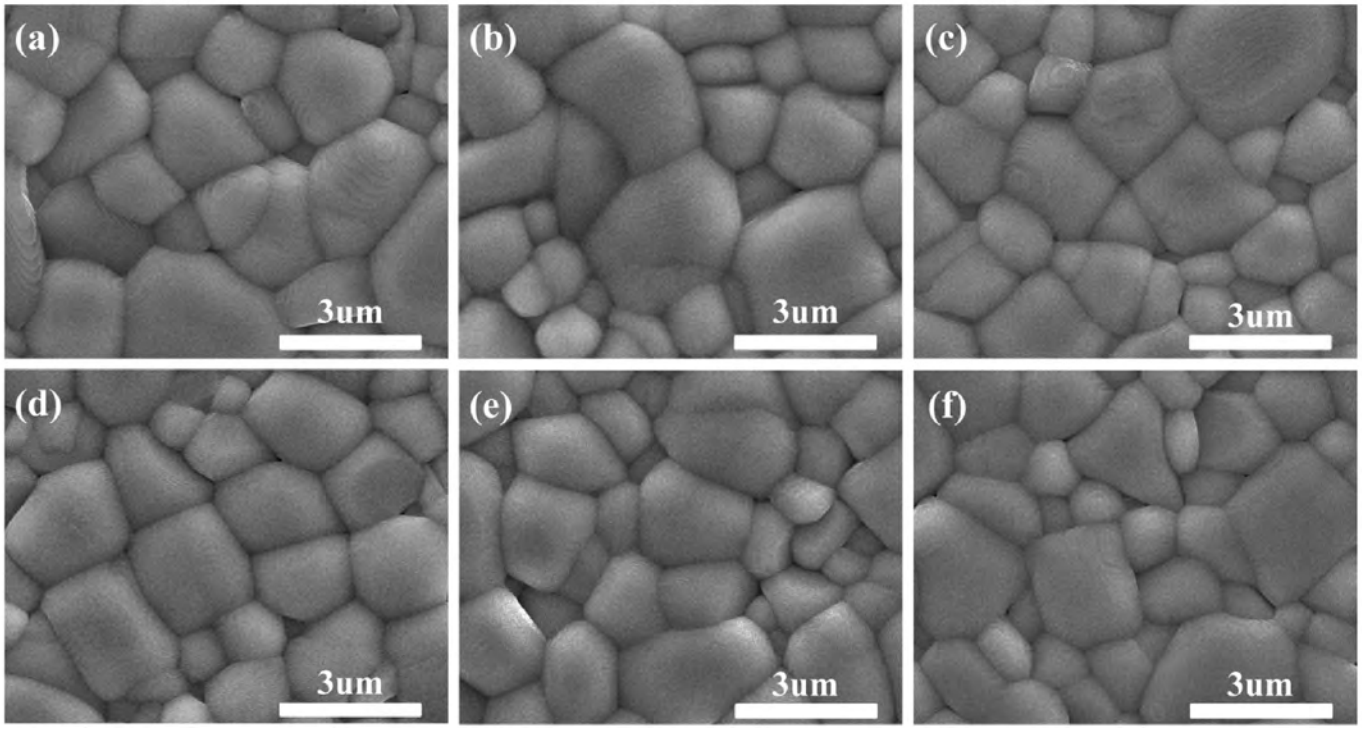

Fig. 2. SEM images of the surfaces of $(1-x)CaTiO_3-x(Li_{0.5}Sm_{0.5})TiO_3$ ($0.70 \le x \le 0.80$) ceramics after hot corrosion treatment: (a) $x = 0.70$; (b) $x = 0.72$; (c) $x = 0.74$; (d) $x = 0.76$; (e) $x = 0.78$; (f) $x = 0.80$.

The τ_f value of the ceramics as a function of x value is shown in Fig. 3(c). The τ_f value decreases monotonously from +66.7 ppm/°C to −10.3 ppm/°C as x increases from 0.70 to 0.80. In addition, at $x = 0.78$, a near-zero τ_f value of +1.6 ppm/°C was obtained. Compared to $CaTiO_3$ which is with a positive τ_f value of +800 ppm/°C, $(Li_{0.5}Sm_{0.5})TiO_3$ have a negative τ_f value of −260 ppm/°C [4]. As a result, theoretically the τ_f value of the CLST system can be effectively changed in the range from −260 to +800 ppm/°C by compositional tailoring. Therefore, a compromise was made and the optimal microwave dielectric properties were achieved for the $0.22CaTiO_3$-$0.78(Li_{0.5}Sm_{0.5})TiO_3$ ceramics with $\varepsilon_r = 109.4$, $Q \times f = 4698$ GHz, and $\tau_f = +1.6$ ppm/°C. Compared to other material systems with a high dielectric constant in recent years [12,25,26], the CLST ceramics have better microwave dielectric properties, including a higher dielectric constant and a near zero resonant frequency temperature coefficient.

To investigate the relationships between the vibrational modes and the microwave dielectric properties of the CLST ceramics, Raman spectra, infrared reflection spectra, and group theory were employed. It has been proved that $CaTiO_3$ has an orthorhombic

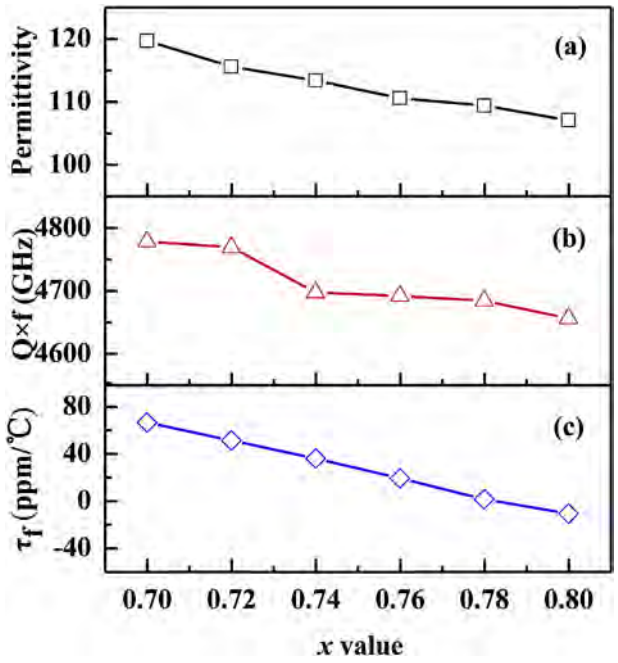

Fig. 3. Microwave dielectric properties of $(1-x)CaTiO_3-x(Li_{0.5}Sm_{0.5})TiO_3$ ($0.70 \le x \le 0.80$) ceramics as a function of x value.

perovskite structure with a space group *Pmna*. The phonons at the Γ-point of the first Brillouin zone can be described in terms of the irreducible representations of the D_{2h} point group:

$$\Gamma = 7A_g + 5B_{1g} + 7B_{2g} + 5B_{3g} + 8A_u + 10B_{1u} + 8B_{2u} + 10B_{3u} \quad (2)$$

24 Raman active ($7A_g$, $5B_{1g}$, $7B_{2g}$, $5B_{3g}$) and 25 infrared active ($7B_{1u}$, $9B_{2u}$, $9B_{3u}$) modes are to be expected [27,28]. However, in reality, not all of these bands can be observed. It is possible that many of the predicted bands are hidden behind other intense bands, and may overlap or involve very low changes in polarizability, preventing their bands from being seen in the spectrum [27].

Fig. 4 shows the room-temperature Raman spectra of the CLST ceramics in the range of 100–1000 cm^{-1}. As indicated by previous XRD analysis, the CLST ceramics possess an orthorhombic perovskite structure, which is identical to the structure of orthorhombic $CaTiO_3$. Therefore, CLST and $CaTiO_3$ should have similar vibrational spectra. Clearly, in the Raman spectra of the CLST samples, eight Raman bands can be observed, at 152, 225, 287 355, 479, 545, 767, and 829 cm^{-1}, respectively. The broad and weak bands at 829 and 767 cm^{-1} are associated with lattice defects, and the band at 545 cm^{-1} is close to that of pure Ti–O symmetric stretching vibration [29]. The 479 cm^{-1} band may be assigned to Ti–O torsional modes (bending or internal vibration of the oxygen cage). The bands in the region of 355–225 cm^{-1} should be attributed to the modes associated with rotations of the oxygen cage, and that at 152 cm^{-1} to the motion of A-site ions [30,31].

To clearly observe the changes in the Raman spectra of the samples with an increase in the x value, the peaks were fitted by a Lorentzian model. Fig. 5 shows the Raman spectra of CLST ($x = 0.70$ and 0.80) ceramics de-convoluted into eight peaks. The wave number and full width at half maximum (FWHM) of the de-convoluted peaks of these two samples are listed in Table 1. The Raman spectra of the other samples were also fitted by the Lorentzian model, and the frequencies and the FWHM values of all the samples obtained from the fitting treatment are shown in Fig. 6. We

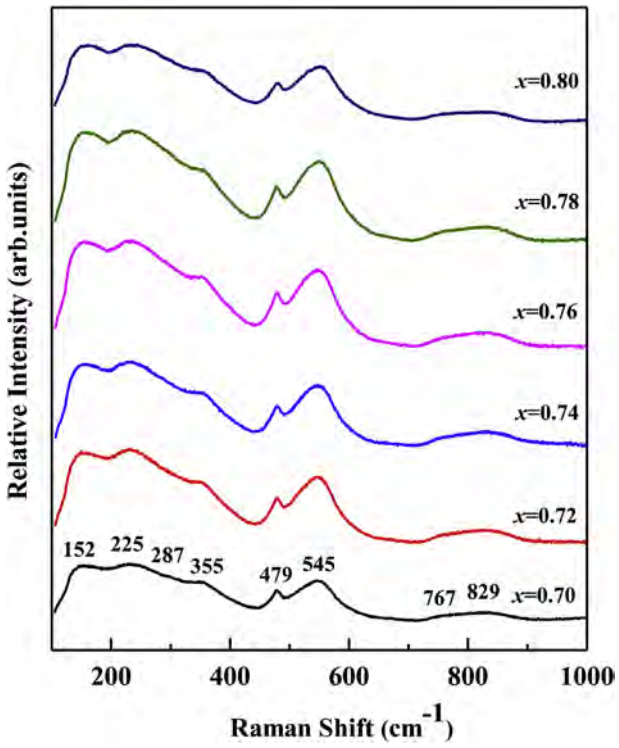

Fig. 4. Raman spectra of $(1-x)CaTiO_3-x(Li_{0.5}Sm_{0.5})TiO_3$ ($0.70 \le x \le 0.80$) ceramics.

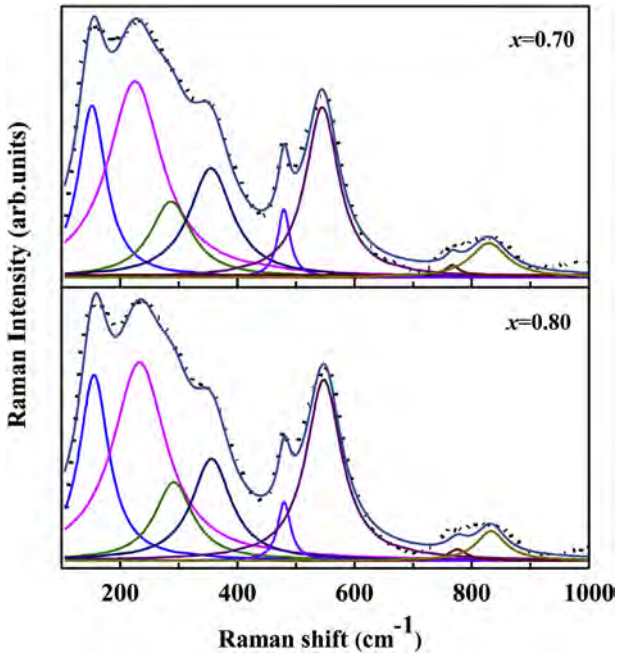

Fig. 5. Raman spectra of $(1-x)CaTiO_3-x(Li_{0.5}Sm_{0.5})TiO_3$ ($x = 0.70, 0.80$) ceramics. Black dots are experimental data, and solid lines are the Lorentz modes.

focus on the vibrational modes of the three strongest peaks (mode-1, mode-2, and mode-6). As the x value increases, there is no obvious variation in the frequencies of these three vibration modes, as is shown in Fig. 6(a). Additionally, from Fig. 6(b), the FWHM values of mode-2 and mode-6 vary randomly with an increase in the x value, expect the vibrational mode at 152 cm^{-1} (mode-1). The FWHM values of mode-1 showed a monotonous increase with an

Table 1
Parameters of the Lorentzian model obtained by fitting the Raman spectra of $(1-x)CaTiO_3-x(Li_{0.5}Sm_{0.5})TiO_3$ ($x = 0.70, 0.80$) ceramics.

Mode	Vibration mode	$x = 0.70$		$x = 0.80$	
		Wavenumber(cm^{-1})	FWHW	Wavenumber(cm^{-1})	FWHW
1	motion of A-site ions	152.0	58.3	155.5	61.4
2	O–Ti–O bending mode	225.4	113.0	233.0	111.0
3	O–Ti–O bending mode	286.7	85.7	291.5	79.0
4	O–Ti–O bending mode	355.0	89.6	356.0	81.4
5	Ti–O torsional mode	479.4	25.5	479.9	26.5
6	symmetric stretching mode of TiO_6 octahedral	544.9	69.1	547.6	73.4
7	lattice defect	766.8	26.4	775.5	39.7
8	lattice defect	829.4	77.2	832.8	60.2

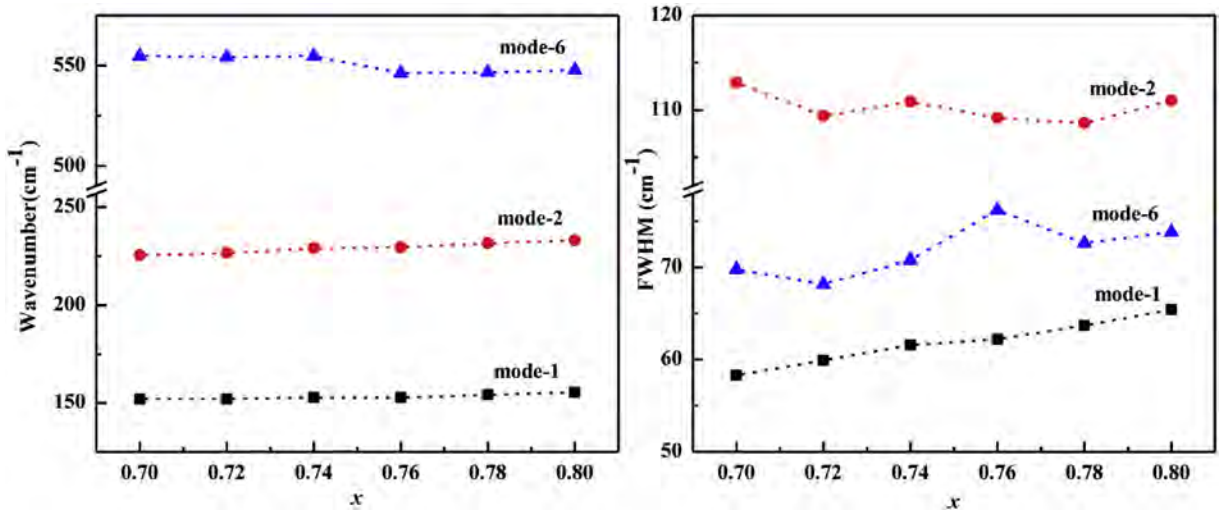

Fig. 6. Raman mode parameters-frequencies and FWHM values of $(1-x)CaTiO_3-x(Li_{0.5}Sm_{0.5})TiO_3$ ($0.70 \le x \le 0.80$) ceramics obtained by the Lorentz model.

increase in the x value, which is due to the decrease in the order degree of A-site ions (i.e., Li^+, Sm^{3+}, and Ca^{2+}). While the disordered distribution of A-site ions have considerable effects on the dielectric behaviors of microwave dielectric ceramics, because the disordered A-site ions may break the periodic arrangement of charges and then increase the dielectric losses [32,33]. In this study, the disordered distribution of A-site ions in the CLST system resulted in the broadening of the Raman spectra of mode-1 and an increase in its FWHM value, which deteriorates the $Q \times f$ values of CLST ceramics as the x value increases.

Fig. 7 illustrates the infrared reflection spectra of the CLST samples ranging from 50 to 1200 cm^{-1}. The infrared reflection spectra were fitted with 12 resonant modes using the classical oscillator model. The fitted results (black lines) are quite consistent with the measured spectra (red circles). The phonon parameters obtained from the fitting treatment of the infrared reflection spectra of the CLST ceramics are listed in Table 2. The infrared reflection spectra of the CLST ceramics can be divided into three wavenumber regions, corresponding to those for a simple perovskite structure [34]. The modes below 150 cm^{-1} are due to the external vibration mode of the A-site cations. The modes in the range of 150–500 cm^{-1} should be ascribed to Ti–O–Ti bending modes, and the modes above 500 cm^{-1} should be attributed to Ti–O stretching modes [28]. These classifications are basically consistent with Raman results.

According to the Fresnel equation (Eq. (3)), the dielectric function $\varepsilon^*(\omega)$ is associated with the infrared reflectance $R(\omega)$; thus, the complex dielectric response of the CLST ceramics can be obtained from the fitting of the infrared spectra using the Lorentz oscillator

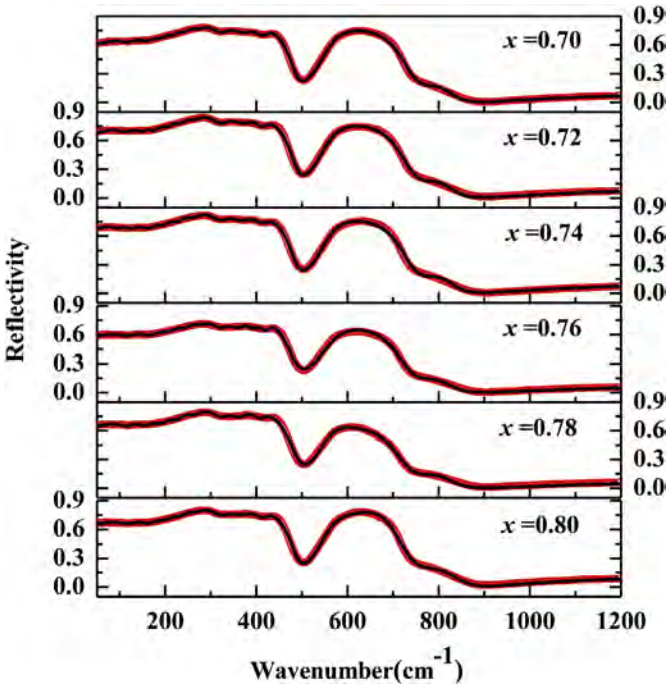

Fig. 7. Measured (red circles) and fitted (black lines) infrared reflection spectra of $(1-x)CaTiO_3-x(Li_{0.5}Sm_{0.5})TiO_3$ ($0.70 \le x \le 0.80$) ceramics. (For interpretation of the references to colour in this figure legend, the reader is referred to the web version of this article.)

Table 2
Phonon parameters obtained from fitting the infrared reflection spectra of (1-x)$CaTiO_3$-x($Li_{0.5}Sm_{0.5}$)TiO_3 (0.70 < x < 0.80) ceramics.

Mode	x = 0.72 ε_∞ = 4.84				x = 0.74 ε_∞ = 5.05				x = 0.76 ε_∞ = 5.54				x = 0.78 ε_∞ = 4.65			
	ω_{oj}	ω_{pj}	γ_j	$\triangle\varepsilon_j$	ω_{oj}	ω_{pj}	γ_j	$\triangle\varepsilon_j$	ω_{oj}	ω_{pj}	γ_j	$\triangle\varepsilon_j$	ω_{oj}	ω_{pj}	γ_j	$\triangle\varepsilon_j$
1	94	578	51	**37.8**	93	569	68	**37.4**	94	574	80	**37.3**	92	546	54	**35.2**
2	137	579	43	**17.9**	143	597	59	**17.4**	143	577	51	**16.3**	138	561	46	**16.5**
3	173	551	36	**10.1**	189	681	50	**13.0**	183	530	37	**8.4**	176	558	38	**10.0**
4	201	605	33	**9.1**	223	668	46	**9.0**	213	600	34	**7.9**	206	602	35	**8.5**
5	229	584	35	**6.5**	257	564	55	**4.8**	240	559	34	**5.4**	234	593	36	**6.4**
6	260	464	44	**3.2**	309	340	53	**1.2**	270	532	41	**3.9**	265	483	44	**3.3**
7	322	304	44	**0.9**	372	194	37	**0.3**	316	342	43	**1.2**	316	296	43	**0.9**
8	357	210	38	**0.3**	402	110	24	**0.1**	345	305	41	**0.8**	344	241	39	**0.5**
9	389	155	33	**0.2**	421	88	17	**0.04**	377	268	46	**0.6**	377	234	44	**0.4**
10	418	127	23	**0.1**	548	575	53	**1.1**	416	206	39	**0.2**	415	161	34	**0.2**
11	550	616	52	**1.3**	689	380	56	**0.3**	556	702	46	**1.6**	552	647	51	**1.4**
12	782	248	104	**0.1**	778	329	159	**0.2**	785	292	107	**0.1**	783	254	99	**0.1**

The bold numbers are calculated values, which need to be emphasized.

model (Eq. (4)).

$$R(\omega) = \left|\frac{1-\sqrt{\varepsilon^*(\omega)}}{1+\sqrt{\varepsilon^*(\omega)}}\right|^2 \tag{3}$$

$$\varepsilon^*(\omega) = \varepsilon_\infty + \sum_{j=1}^{n} \frac{\omega_{pj}^2}{\omega_{oj}^2 - \omega^2 - i\gamma_j\omega} \tag{4}$$

where ε_∞ is the high-frequency permittivity caused by the electronic polarization; ω_{pj}, ω_{oj}, and γ_j are the plasma frequency, the eigenfrequency, and the damping coefficient of the j-th Lorentz oscillator, respectively; and n is the number of phonon modes. In the microwave frequency region ($\omega \ll \omega_{pj}$), ε' (Eq. (5)) and tanδ (Eq. (6)) can be derived from the Lorentzian formula. Therefore, the contributions of each phonon to the microwave dielectric properties can be calculated:

$$\varepsilon' = \varepsilon_\infty + \sum_{j=1}^{n} \Delta\varepsilon_j = \varepsilon_\infty + \sum_{j=1}^{n} \frac{\omega_{pj}^2}{\omega_{oj}^2} \tag{5}$$

$$\tan\delta = \frac{\varepsilon''}{\varepsilon'} = \omega \sum_{j=1}^{n} \frac{\Delta\varepsilon_j\gamma_j}{\omega_{oj}^2\left(\varepsilon_\infty + \sum_{j=1}^{n}\Delta\varepsilon_j\right)} \tag{6}$$

where $\triangle\varepsilon_j$ is the contribution of a phonon to the permittivity from the j-th Lorentz oscillator. In the CLST ceramics, the value of $\triangle\varepsilon_j$ represents the mode that contributes to the permittivity.

The complex dielectric responses (ε' and ε'') of the CLST ceramics obtained from the fitting treatment of the infrared reflection spectra and corresponding experimental microwave data are shown in Fig. 8. The calculated permittivities are slightly lower than the measured ones in the microwave range. Meanwhile, the calculated dielectric losses are quite consistent with the values measured using the $TE_{01\delta}$ method. Therefore, it can be concluded that the dielectric polarization of the CLST ceramics in the microwave region is dominated by the phonons in the infrared region [20].

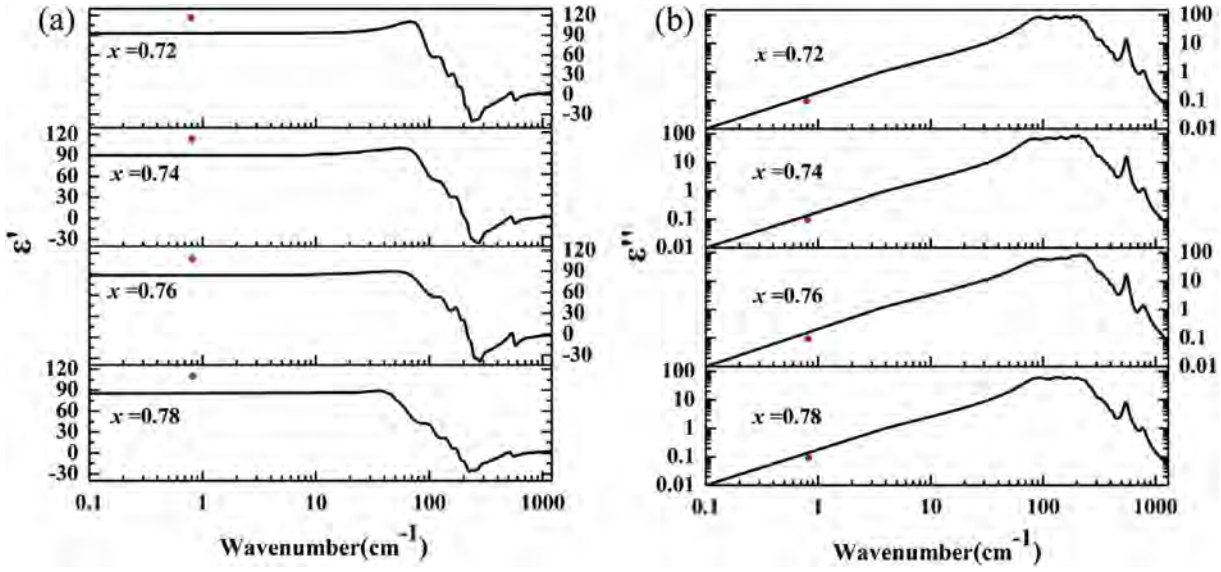

Fig. 8. The real (a) and imaginary (b) parts of the complex dielectric response of (1−x)$CaTiO_3$−x($Li_{0.5}Sm_{0.5}$)TiO_3 (0.70 < x < 0.80) ceramics. Red dots are experimental microwave data; solid lines are the results from fitting the infrared spectra. (For interpretation of the references to colour in this figure legend, the reader is referred to the web version of this article.)

Phonon parameters obtained from the fitting of the infrared reflection spectra of the CLST ceramics are given in Table 2. The permittivity contributions of the modes at low frequencies, below 150 cm^{-1}, are much larger than that of other modes in the CLST ceramics, and the permittivity contributions decrease with an increase in the x value. In addition, the sum of the contribution of the vibrational modes to the dielectric constant also decreases with increasing x value. Therefore, the permittivity of the CLST ceramics decreased as the x value increased, which is consistent with the measured results. In this study, the external vibration modes at low frequencies related to the A-site ions play an important role in the microwave dielectric properties of the CLST ceramics. When the x value increased, the permittivity contributions of the external vibration modes at low frequencies related to the A-site cations decreased. This took a significant effect on the decrease in the dielectric constant of the CLST ceramics. It indicates that the dielectric properties of the CLST materials can be effectively tailored by A-site substitutions.

4. Conclusion

(1-x)$CaTiO_3$-x($Li_{0.5}Sm_{0.5}$)TiO_3 ($0.7 \leq x \leq 0.8$) ceramics were prepared by the conventional solid-state reaction method. All ceramic samples demonstrate a pure orthorhombic perovskite structure, and there is no apparent difference in morphology. The microwave dielectric properties of the samples were studied by varying the composition. As the x value increases, the permittivity and $Q \times f$ value decrease, and the τ_f value changes from positive into negative. At $x = 0.78$, the optimal microwave dielectric properties of $\varepsilon_r = 109.4$, $Q \times f = 4698$ GHz, and $\tau_f = 1.6$ ppm/°C were obtained. The vibrational properties of the A-site ions of the CLST ceramics were investigated by Raman and infrared spectra analyses. As revealed by the Raman results, the $Q \times f$ value decreased with an increase in the x value as a result of the lowered order degree of the A-site ions. Additionally, the infrared reflectance spectra indicate that the permittivity of the CLST ceramics is strongly dependent on the external vibration modes at low frequencies (i.e., <150 cm^{-1}), related to the A-site cations. This result implies that A-site substitutions could be an effective method to tailor the properties of CLST ceramic materials.

Acknowledgements

This work was supported by the National Science Foundation of China (11774083). The authors would like to thank the administrators in the IR beamline workstation of National Synchrotron Radiation Laboratory (NSRL), University of Science and Technology of China, for their help in the IR measurements.

References

[1] I.M. Reaney, D. Iddles, J. Am. Ceram. Soc. 89 (2006) 2063–2072.
[2] B. Ullah, W. Lei, Z.-Y. Zou, X.-H. Wang, W.-Z. Lu, J. Alloy. Compd. 695 (2017) 648–655.
[3] Z.-Y. Shen, Q.-G. Hu, Y.-M. Li, Z.-M. Wang, W.-Q. Luo, Y. Hong, Z.-X. Xie, R.-H. Liao, X. Tan, J. Am. Ceram. Soc. 96 (2013) 2551–2555.
[4] H. Takahashi, Y. Baba, K. Ezaki, Y. Okamoto, K. Shibata, K. Kuroki, S. Nakano, Jpn. J. Appl. Phys. 30 (1991) 2339.
[5] J. Mercurio, M. Manier, B. Frit, Ferroelectrics 127 (1992) 35–40.
[6] K. Ezaki, Y. Baba, H. Takahashi, K. Shibata, S. Nakano, Jpn. J. Appl. Phys. 32 (1993) 4319.
[7] J. Kato, H. Kagata, K. Nishimoto, Jpn. J. Appl. Phys. 30 (1991) 2343.
[8] E.S. Kim, K.H. Yoon, J. Eur. Ceram. Soc. 23 (2003) 2397–2401.
[9] K. Yan, M. Fujii, T. Karaki, M. Adachi, Jpn. J. Appl. Phys. 46 (2007) 7105–7107.
[10] J. Li, Y. Han, T. Qiu, C. Jin, Mater. Res. Bull. 47 (2012) 2375–2379.
[11] Y.M. Li, T.T. Song, F. Hu, R.H. Liao, B. Zhang, Adv. Mater. Res. 105–106 (2010) 238–241.
[12] F.-f. Gu, G.-h. Chen, C.-l. Yuan, C.-r. Zhou, T. Yang, Y. Yang, Mater. Res. Bull. 61 (2015) 245–251.
[13] A. Dias, L.A. Khalam, M.T. Sebastian, M.M. Lage, F.M. Matinaga, R.L. Moreira, Chem. Mater. 20 (2008) 259–269.
[14] F. Shi, H. Dong, Dalton Trans. 40 (2011) 6659–6667.
[15] D. Zhou, L.-X. Pang, H. Wang, J. Guo, X. Yao, C.A. Randall, J. Mater. Chem. 21 (2011) 18412.
[16] K. Wakino, M. Murata, H. Tamura, J. Am. Ceram. Soc. 69 (1986) 34–37.
[17] H. Zheng, G.D.C. Csete de Györgyfalva, R. Quimby, H. Bagshaw, R. Ubic, I.M. Reaney, J. Yarwood, J. Eur. Ceram. Soc. 23 (2003) 2653–2659.
[18] W.-B. Li, D. Zhou, H.-H. Xi, L.-X. Pang, X. Yao, N. Alford, J. Am. Ceram. Soc. 99 (2016) 2083–2088.
[19] W.-B. Li, D. Zhou, D. Guo, L.-X. Pang, G.-H. Chen, Z.-M. Qi, Q.-P. Wang, H.-C. Liu, J. Alloy. Compd. 694 (2017) 40–45.
[20] J. Guo, C.A. Randall, D. Zhou, G. Zhang, C. Zhang, B. Jin, H. Wang, J. Eur. Ceram. Soc. 35 (2015) 4459–4464.
[21] R.D. Shannon, Acta Crystallogr. 32 (1976) 751–767.
[22] H.-H. Xi, D. Zhou, H.-D. Xie, B. He, Q.-P. Wang, N. Alford, J. Am. Ceram. Soc. 98 (2015) 587–593.
[23] Z.-M. Dou, J. Jiang, G. Wang, F. Zhang, T.-J. Zhang, Ceram. Int. 42 (2016) 6743–6748.
[24] F. Liu, X.-Y. Liu, C.-L. Yuan, J.-J. Qu, G.-H. Chen, C.-R. Zhou, F. Liu, J. Eur. Ceram. Soc. 35 (2015) 2091–2098.
[25] Z.-X. Fang, B. Tang, F. Si, S.-R. Zhang, J. Alloy. Compd. 693 (2017) 843–852.
[26] H.-T. Chen, B. Tang, P. Fan, M. Wei, S.-R. Zhang, Ceram. Silikáty 61 (2017) 1–5.
[27] H. Zheng, I.M. Reaney, G.D.C.C. De Gyórgyfalva, R. Ubic, J. Yarwood, M.P. Seabra, V.M. Ferreira, J. Mater. Res. 19 (2003) 488–495.
[28] K.W. Sup, Y.K. Hyun, K.E. Soo, J. Am. Ceram. Soc. 83 (2000) 2327–2329.
[29] S.Y. Wu, Y. Li, X.M. Chen, J. Phys. Chem. Solids 64 (2003) 2365–2368.
[30] T. Hirata, K. Ishioka, M. Kitajima, J. Solid State Chem. 124 (1996) 353–359.
[31] U. Balachandran, N.G. Eror, Solid State Commun. 44 (1982) 815–818.
[32] E. Schlömann, Phys. Rev. 135 (1964) 413–419.
[33] H. Tamura, J. Eur. Ceram. Soc. 26 (2006) 1775–1780.
[34] C.H. Perry, B.N. Khanna, G. Rupprecht, Phys. Rev. 135 (1964) A408–A412.